Proc. Natl. Acad. Sci. USA
Vol. 87, pp. 9703–9707, December 1990
Neurobiology

Neuropathological changes in transgenic mice carrying copies of a transcriptionally activated *Mos* protooncogene

(*Mos* expression/oncogene/transgene)

FRIEDRICH PROPST*†, MICHAEL P. ROSENBERG*‡, LINDA C. CORK§, ROBERT M. KOVATCH¶, STEVEN RAUCH‖, HEINER WESTPHAL**, JASPAL KHILLAN††, NICHOLAS T. SCHULZ*, GEORGE F. VANDE WOUDE*‡‡, AND PAUL E. NEWMANN§§

*ABL–Basic Research Program, National Cancer Institute–Frederick Cancer Research and Development Center, P.O. Box B, Frederick, MD 21702; §Division of Comparative Medicine, The Johns Hopkins University School of Medicine, 720 Rutland Avenue, Baltimore, MD 21205; ¶Pathology Associates, Inc., Worman's Mill Court, Frederick, MD 21701; ‖Massachusetts Eye and Ear Infirmary, Department of Otolaryngology, Harvard Medical School, 243 Charles Street, Boston, MA 02115; **Laboratory of Molecular Genetics, National Institutes of Child Health and Human Development, National Institutes of Health, Bethesda, MD 20892; ††Thomas Jefferson University, Jefferson Alumni Hall, 1020 Locust Street, Philadelphia, PA 19107; and §§Neurology Research, Children's Hospital, 300 Longwood Avenue, Boston, MA 02115

Communicated by George Klein, September 25, 1990

ABSTRACT **Independent transgenic mouse lines carrying the mouse *Mos* protooncogene linked to a retroviral transcriptional control sequence display behavioral abnormalities including circling, head tilting, and head bobbing. This dominant phenotype shows various degrees of penetrance in different transgenic founder animals and lines. Neuronal and axonal degeneration, gliosis, and inflammatory infiltrates are found in all transgenic mouse lines in which behavioral traits are present. Recordings of auditory-evoked potentials in mice of one of these lines demonstrate that transgenic mice are deaf; in these mice spiral ganglia degenerate and most of the cochlear hair cells are absent. By using an S1 nuclease protection assay, we have detected RNA expression of the transgene in all tissues examined and, in particular, at high levels in brain. *In situ* hybridization experiments show that *Mos* expression can be detected in specific areas of the central nervous system. Lesions are present in areas with demonstrable overexpression of *Mos*.**

In normal mouse tissues expression of the *Mos* protooncogene is tightly regulated. Low levels of *Mos* mRNA have been detected in adult brain, kidney, mammary gland, and epididymis, as well as in 18- to 19-day mouse embryos (1). Higher levels of *Mos* RNA expression can be detected in gonads of adult mice and several other species (1–9). Gonadal *Mos* expression appears to be confined to germ cells. The *Mos* protooncogene product has been detected in isotopically labeled oocytes of mice (10) and *Xenopus laevis* (9) as well as in testicular spermatocytes by Western blot analysis (11). The Mos protein is essential for oocyte meiotic maturation (9, 10, 12, 13), is a candidate initiator of maturation-promoting factor (14), and is the well-known cytostatic factor responsible for arresting maturing oocytes at metaphase II (15). Herein we describe the effect of overexpression of *Mos* in the central nervous system of transgenic mice.

MATERIALS AND METHODS

Gene Transfer into Fertilized Eggs. Transgenic mice were generated on two backgrounds, FVB/N and (C57BL/6 × C3H/HeNCr)F_2, hereafter termed B6C3F2 (16, 17). Founders and their progeny were identified by Southern blot analysis (18) of tail biopsies using a *Mos*-specific probe.

Histopathology. Tissues for light microscopy were fixed by immersion in 4% (wt/vol) paraformaldehyde; by intracardiac perfusion with a solution of 3.7% (vol/vol) formaldehyde, 5% (vol/vol) acetic acid, and 60% (vol/vol) ethanol; or by immersion in formalin. Paraffin-embedded sections were stained with cresyl violet, Giemsa, periodic acid-Schiff, or hematoxylin and eosin. Perfusion-fixed [3.7% formaldehyde/4% (wt/vol) sucrose] frozen tissues were selectively silver-impregnated by the first method of Fink and Heimer (19). Immunocytochemistry for phosphorylated epitopes of neurofilaments was carried out as described (20) and for glial fibrillary acidic protein (GFAP) using the Dako kit for GFAP.

Tissues for ultrastructural studies were perfused with 2.5% (vol/vol) glutaraldehyde and 1% paraformaldehyde, post-fixed with osmium tetroxide, and embedded in Epon. Semithin (1 μm) sections were stained with toluidine blue. Thin sections for electron microscopy were stained with uranyl acetate.

Animals for temporal bone study were perfused with Heidenhain–Susa fixative. After soft-tissue debridement, the skulls were postfixed, decalcified in trichloracetic acid, and embedded in celloidin. Every fifth 20-μm section was mounted and stained with hematoxylin and eosin.

RNA Expression Analysis. Total RNA from tissues was prepared and analyzed by S1 nuclease protection assays using *Mos*-specific probes A and F as described (1, 21). *In situ* hybridization was carried out using RNA probes labeled with S^{35}-labeled UTP (22) on sections of paraformaldehyde-fixed tissues as described (6, 23).

RESULTS

Lens Opacity and Abnormal Behavior in *Mos* Transgenic Mice. The mouse *Mos* protooncogene plus ≈800 base pairs of sequences upstream to the first ATG were linked to the long terminal repeat of Moloney murine sarcoma virus, and this construct, pTS74 (24), was introduced into the germline of FVB/N (16) and B6C3F2 mice. Stable integration and transmission of the transgene were obtained in three FVB/N lines and four B6C3F2 lines. Table 1 summarizes the phenotypes observed in these transgenic lines. Four of the seven lines (lines 1–4) displayed opacity of the eye lens resulting from a defect in lens-fiber-cell differentiation (16). This phenotype appeared to be fully penetrant in heterozygous and homozygous animals.

The publication costs of this article were defrayed in part by page charge payment. This article must therefore be hereby marked "*advertisement*" in accordance with 18 U.S.C. §1734 solely to indicate this fact.

Abbreviation: GFAP, glial fibrillary acidic protein.

†Present address: Ludwig Institute for Cancer Research, Saint Mary's Hospital Medical School, Norfolk Place, London W2 1PG, U.K.
‡Present address: Department of Molecular Biology, Squibb Institute for Medical Research, P.O. Box 4000, Princeton, NJ 08543.
‡‡To whom reprint requests should be addressed.

Table 1. Description of mice carrying the *Mos* transgene pTS74

Mouse	GB	LO	AB	BL	C/G	TE
Line 1*	FVB/N	+	+	+	1 or 2	+
Line 2*	FVB/N	+	+	+	1 or 2	+
Line 3*	FVB/N	+	+	+	1 or 2	+
Line 4	B6C3F2	+	+	+	1 or 2	+
Line 5A†	B6C3F2	−	−	−	4–6	±‡
Line 5B	B6C3F2	−	−	−	4–6	±‡
Line 6	B6C3F2	−	−	−	2 or 3	−
Founder A	B6C3F2	+	+	+	>10	++
Founder B	B6C3F2	NT	+	NT	5–10	NT
Founder C	B6C3F2	+	+	+	>10	++

Founders were mice that were necropsied at weaning (founder A), died shortly before being weaned (founder B), or were infertile (founder C). GB, genetic background; LO, lens opacity; AB, aberrant behavior; BL, brain lesion; TG, transgene expression; C/G, copies per genome; NT, not tested.

*Details of the lens defects in these transgenics were reported by Khillan *et al.* (16).

†Founder contained two insertions that segregated independently in the progeny, giving rise to the independent lines 5A and 5B.

‡RNA analysis was performed using the founder of these animals, which segregated for two inserts A and B.

Mice from lines 1–4 also displayed behavioral abnormalities that varied in severity and age of onset among the various lines. These abnormalities resemble the behavior observed in so-called "circling" or "inner-ear" mutants. Penetrance of the behavioral traits was incomplete and less severe in heterozygotes and homozygotes of lines 1, 2, and 3, whereas all heterozygotes of line 4 showed behavioral abnormalities before weaning. Circling and head tilting often appeared around weaning; hyperactivity tended to occur later and progressed in severity. The severity of behavioral changes ranged from mice with minimal hyperactivity and head tilting to the most hyperactive circling behavior we have seen in different inner-ear mutations. The circling behavior varied from periodic runs around the perimeter of the cage to rapid pivoting in the center of the cage and to repeated somersaults. Mice transgenic for *Mos*–pTS74 differed from mutant waltzer (*v*) mice in that there was subtle ataxia and tilting of the entire body and head in repose and in motion. Homozygous transgenic mice did not appear to be more likely to show abnormal behavior than heterozygotes, nor was there any evidence that the severity of their syndrome was any different among these groups. To date we have been unable to obtain homozygotes in line 4. Some severely affected transgenic mice of all four lines were infertile, although the ovaries were histologically normal (data not shown). Line 4 was established by transplantation of the founder's ovaries to syngeneic mice.

Three additional B6C3F2 "founder" mice were produced that failed to establish lines because they died before or at weaning (founders A and B) or were infertile (founder C). All three of these transgenic mice displayed behavioral abnormalities. Furthermore, two of the mice examined had lens opacities (Table 1).

Neuropathology of pTS74 Transgenic Mice. Central nervous system lesions seen in the transgenic mice were consistent in their distribution and character and did not seem to be influenced appreciably by the background strain or by whether the mice were homozygous or heterozygous. Conventional histological methods detected neuropathological changes between 2 and 3 months of age, and lesions were characterized by vacuolation of the neuropil (Fig. 1*A*) associated with swollen, degenerating axons within the granule cell layer of the cerebellum, the motor nuclei of the fifth and seventh cranial nerves, the habenular nucleus, and the posterior and ventral nuclei of the thalamus. Electron microscopy confirmed the axonal origin of these vacuoles (Fig. 1*B*).

Degenerative axonal changes were accompanied by an astrocytosis and infiltration of the neuropil and meninges by inflammatory cells, including microglia, lymphocytes, plasma cells, eosinophils, and mast cells (Fig. 1*C*). Infiltrations of mast cells were also in proximity to many apparently normal neurons within the thalamus (Fig. 1*D*). In addition to the axonal changes, argyrophilic fibrillary material distended the perikarya of occasional neurons with enlarged eccentric nuclei in the pyramidal layers of cortex and of thalamic and brain-stem neurons (Fig. 1*E*). The cytoplasm of these neurons was immunoreactive with antibodies directed against phosphorylated epitopes of neurofilaments that can be detected in neuronal perikarya in natural or experimental disease (20). Other cells with large atypical nuclei and abundant nonargyrophilic and eosinophilic cytoplasm were also present. Many of these were astrocytes and were immunoreactive for GFAP and some were binucleate (Fig. 1*F*). Atypical neurons and astrocytes tended to colocalize in the same regions. In some mice there was a marked proliferation of the Bergmann glia surrounding Purkinje cells. Many of these glia had large atypical nuclei (Fig. 1*G*). One mouse had a midline astrocytoma in the anterior hypothalamus.

Axonal degeneration was more widespread than conventional histological methods indicated. By using the Fink–Heimer method for detecting degenerating axons (19), occasional axonal degeneration was detected in transgenic mice as early as 1 month of age and increased in frequency and distribution with age (Fig. 1*H*). Axonal degeneration was detected in various thalamic regions, including ventral and posterior thalamus, superior and inferior colliculi, subcortical cerebellum, superior cerebellar peduncle, fasciculus retroflexus, and other brainstem tracts, fiber bundles of the striatum, and the deep cortical layers.

The neuropathological changes seen with conventional stains in the thalamus and brain stem increased in severity with age. Between 4 and 5 months of age, there was bilaterally symmetrical frank malacia and encephalitis of the thalamus and the region adjacent to the mammillary recess and third ventricle (Fig. 1*I*).

One of the most striking features was an intense inflammation of the choroid plexus within the lateral ventricle. The normal architecture of the choroid plexus of the lateral ventricles and the ventricular space was virtually obliterated by a massive infiltration of lymphocytes, plasma cells, neutrophils, eosinophils, and mast cells. Wide cuffs of lymphoid cells encircled vessels within the choroid plexus and formed structures similar to germinal centers (Fig. 1*J*). Occasional syncytial cells were also present. The severe inflammatory process extended into the adjacent neuropil; axons were replaced by sheets of gemistocytes (some of which were binucleate), gitter cells, and mononuclear cells. Large atypical neurons and astrocytes were scattered within the neuropil of the thalamus and hippocampus adjacent to this intense encephalitic process.

***Mos* Transgene RNA in Specific Cells of the Central Nervous System.** We have reported that *Mos* is expressed at low levels in the brain of adult mice (1). In brain tissues of 16-day and 19-day fetuses, we detected Mos transcripts in total RNA by S1 nuclease protection analyses (Fig. 2*A*, lanes 3–6). In contrast, high levels of Mos transcripts were found in the brain of adult transgenic mice (16) (Fig. 2*B*) and in the brain and other tissues of founder A (Fig. 2*C*). Other transgenic animals on the B6C3 background that have no apparent brain phenotype showed low (line 5) or undetectable (line 6) levels of transgene RNA expression in the brain (Fig. 2*D*). Note that probe A detects a 480-base band in normal testis RNA (Fig. 2*C*, lane 3) but a 530-base band in RNA from tissues of transgenic mice (Fig. 2*B–D*), indicating that the Mos transcripts detected in transgenic tissues are transcribed from the transgene and not the endogenous *Mos* locus.

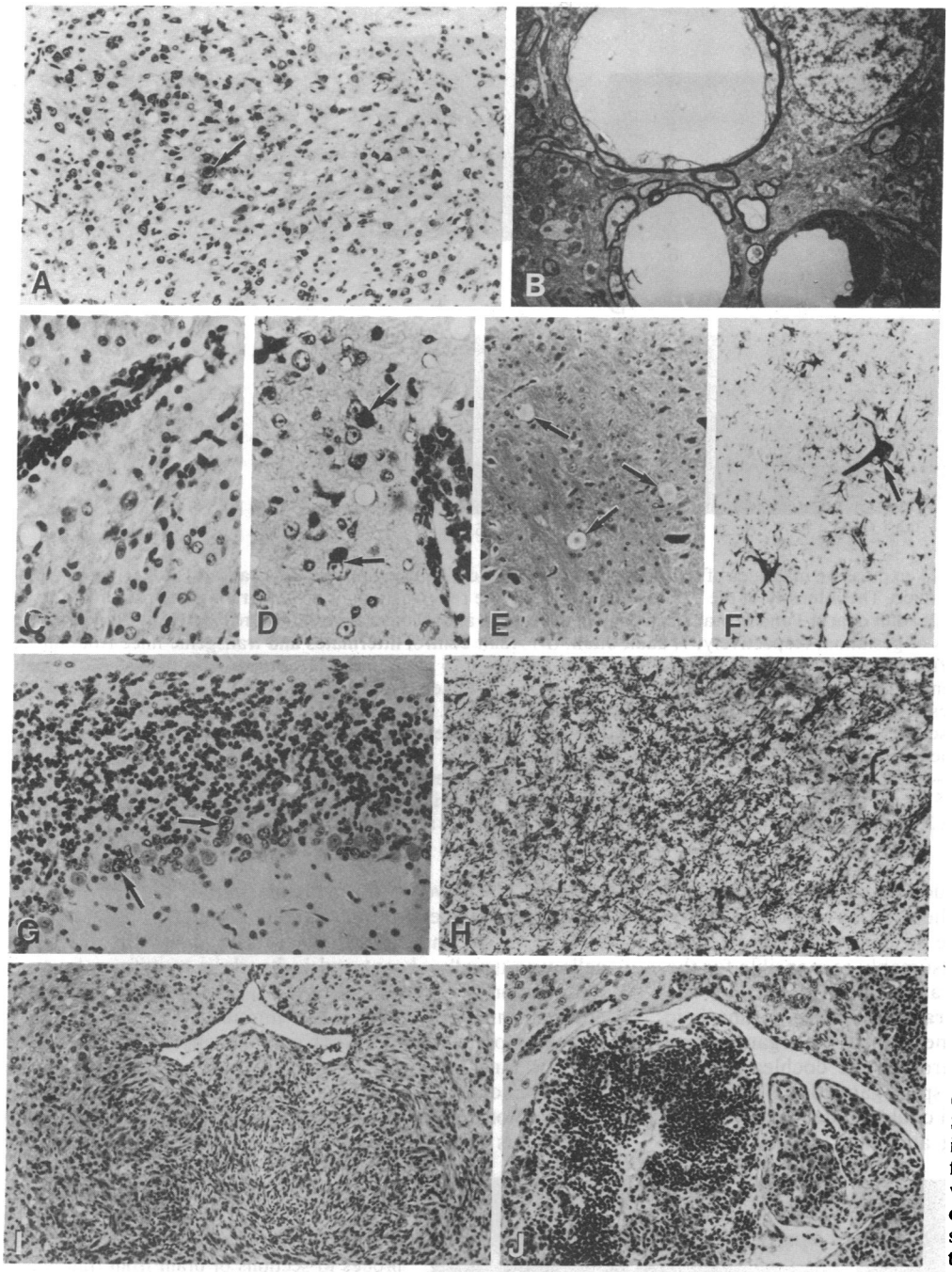

FIG. 1. Histopathology of brains from *Mos* transgenic mice. (*A*) Vacuolation of the posterior nucleus of the thalamus (cresyl violet; ×130). One of the earliest lesions noted was the vacuolation of the neuropil associated with degeneration of neurons. Some large cells contained abnormal nuclei (arrow). (*B*) Two electron-lucent vacuoles, one of which is surrounded by a myelin sheath (×2600). This distended degenerating axon contains only a remnant of axoplasm. (*C*) Perivascular infiltrate and gliosis involving the thalamus adjacent to the lateral ventricle [hematoxylin and eosin (H&E); ×275]. (*D*) Perivascular cuff of mononuclear cells and mast cells (Giemsa; ×275). Arrows indicate mast cells that have infiltrated into the parenchyma and are adjoined to neurons. (*E*) Swollen neurons of the fifth cranial nerve in a 3.5-month-old transgenic mouse from line 4 (H&E; ×130). Some swollen neurons contained phosphorylated epitopes of neurofilaments (arrows). (*F*) Atypical hyperplastic astrocytes immunoreactive for GFAP (×110). Some large atypical cells are clearly astrocytic in origin and their cytoplasm contained GFAP. An occasional binucleate cell (arrow) is also present. (*G*) Cerebellum with proliferation of Bergmann glia (H&E; ×180). In some transgenic mice, Purkinje cells were atrophic and reduced in number; proliferation of Bergmann glia occurred, and many had abnormal nuclei (arrows). (*H*) Ventral thalamus from 4-month-old transgenic mouse from line 3 showing axonal degeneration as revealed by short disrupted fibers (silver impregnation; ×130). (*I*) Severe proliferation of glial cells intermixed with mononuclear inflammatory cells beneath the third ventricle (H&E; ×45). (*J*) Choroid plexus obliterated by a massive mixed inflammatory cell infiltrate (H&E; ×105).

By *in situ* hybridization elevated Mos RNA expression was localized to specific areas and cell types in the brains of circling transgenic mice of lines 3 and 4. Hybridization specificity with a complementary ^{35}S-labeled Mos RNA probe was determined by comparing adjacent sections hybridized with a control sense Mos RNA probe. Only hybridization with the complementary Mos probe resulted in the deposition of silver grains and demonstrated the presence of Mos transcripts (Fig. 3). Numerous labeled perikarya were observed within the hippocampal formation and subicular complex (Fig. 3); silver grains were also localized over pyramidal neurons and cells in the molecular layer but not over the fascia dentata. The entorhinal cortex contained numerous positive cells in the molecular layer and in a few positive cells in deeper layers. Neocortical areas of the telencephalon showed only scattered positive cells. The fornix also contained clusters of silver grains, suggesting hybridization to cellular profiles. Densely grouped clusters of silver grains were noted in the diencephalon in the habenula, pineal body, posterior thalamic nucleus, lateral posterior thalamic nucleus, ventral posterior thalamic nuclei, anteroventral thalamic nuclei, zona incerta, fields of Forel, preoptic area, dorsal medial hypothalamic nucleus, arcuate nucleus, and lateral hypothalamus (Fig. 3*A*). Within the cerebellum, Purkinje cells were labeled, as were a few cells in the deep cerebellar nuclei and possibly Bergmann glia (Fig. 3*B*). In the brain stem, large neurons in the motor nucleus of the fifth cranial nerve, the facial nucleus, and the lateral vestibular nucleus were clearly labeled (Fig. 3*B*). The substantia nigra, red nucleus, nuclei of the lateral lemnisci, and deep gray layers of the superior and inferior colliculi also contained clusters of silver grains in cellular profiles (Fig. 3*B*). No similar labeling pattern could be detected in corresponding sections of normal littermates (data not shown). However, the hippocampal formation and subicular complex contained numerous cellular profiles that were slightly positive (data not shown).

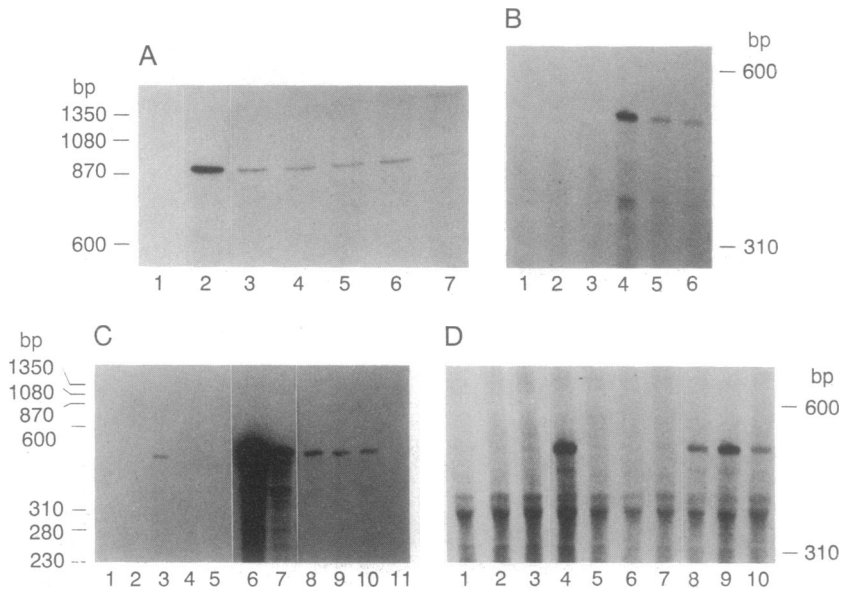

FIG. 2. S1 nuclease analysis of RNA expression in tissues of transgenic and control mice, by using probes F (*A*) and A (*B–D*) (1). (*A*) Adult and embryonic control C57BL/6NCr mice. The intensity of the 925-base band reflects the relative amount of Mos transcripts present in 25 μg of total RNA. Lanes: 1, yeast tRNA; 2, adult ovary; 3 and 4, brain from male fetuses at 16 and 19 days of gestation, respectively; 5 and 6, brain from female fetuses at 16 and 19 days of gestation, respectively; 7, adult brain. (*B*) Adult control littermates and transgenic mice from line 4. The intensity of the 530-base band reflects the relative amount of Mos transcripts present in 25 μg of total RNA prepared from tissues of a male control littermate (lanes 1–3) and a female transgenic mouse (lanes 4–6) at 25 days of age. Lanes: 1 and 4, brain; 2 and 5, kidney; 3 and 6, liver. (*C*) Adult control C57BL/6NCr (lanes 1–5) and founder A (lanes 6–10) mice at 22 days of age. Lanes: 1 and 6, brain; 2 and 7, kidney; 3, testis; 4 and 9, lung; 5 and 10, heart; 8, muscle; 11, yeast tRNA. Total RNA (25 μg) was used from each tissue except for lanes 4 and 9 (4 μg), 5 and 10 (1 μg), 7 (18 μg), and 8 (1.5 μg). The probe detects a 480-base band in normal testis RNA and a 530-base band in RNA from transgenic tissues. (*D*) Adult control littermate (lanes 1–3) and transgenic mouse (lane 4) from line 4 and founder mice from line 5 (lanes 8–10) and line 6 (lanes 5–7) are shown. The intensity of the 530-base band reflects the relative amount of Mos transcripts present in 25 μg of total RNA prepared from brain (lanes 1, 4, 5, and 8), liver (lanes 2, 6, and 9), and kidney (lanes 3, 7, and 10). Smaller bands are due to background observed in this particular experiment. bp, Base pairs.

From these analyses we conclude that Mos transcripts are expressed in transgenic mice in the neurons and astrocytes in localized areas of the brain where the central nervous system lesions are observed and are presumably responsible for the cells undergoing axonal degeneration.

Hair-Cell Disorder in *Mos* Transgenic Mice. Transgenic mice from line 3 had severe degeneration of the organ of Corti with loss of hair cells in all turns of the cochlea, loss of supporting cells, and atrophy of spiral ganglion cells (Fig. 4). Occasional inner-hair-cell nuclei could be identified within a collapsed mound of supporting and pillar cells where the organ of Corti would normally be found, but the tectorial membrane was never noted to be in contact with this mound of cells. In the middle and basal turns, even this mound of cells was usually absent and in its place a uniform layer of flattened or low cuboidal cells was indistinguishable from the adjacent inner sulcus cells. The limbus, normally a rounded convex mound with Reissner's membrane arising along the convex surface, was deformed throughout all turns of the mutant cochlea. The "convex" surface was replaced by a flattened or concave region leaving a deep trough between the limbus and the modiolar end of Reissner's membrane

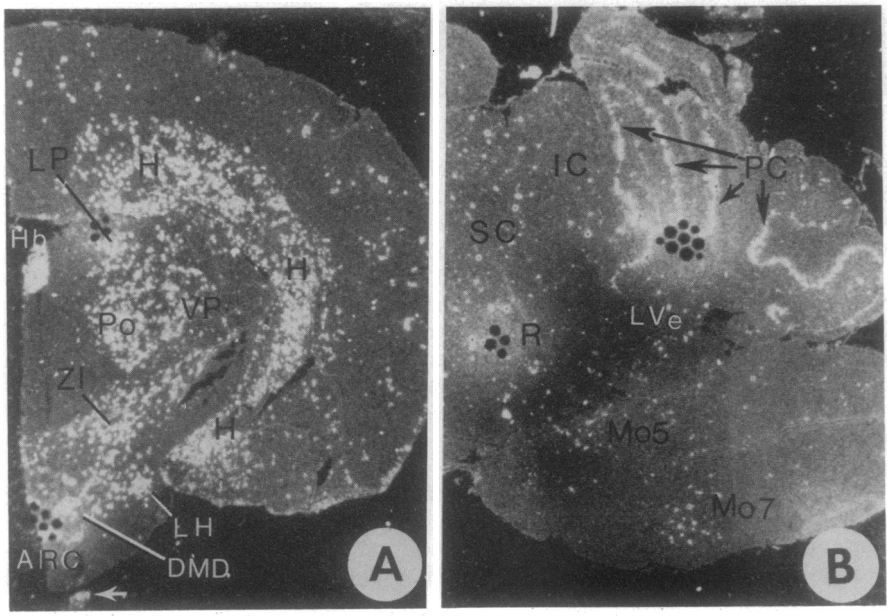

FIG. 3. *In situ* hybridization of Mos probes to sections of brain from transgenic mice. (*A*) Dark-field photomicrograph of coronal section of the forebrain from a 25-day-old transgenic mouse from line 4 (×7.5). The most intense staining is evident in the hippocampal formation (H), habenula (Hb), posterior thalamic nucleus (Po), lateral posterior thalamic nucleus (LP), ventroposterior thalamic nucleus (VP), zona incerta (ZI), lateral hypothalamus (LH), dorsomedial hypothalamic nucleus (DMD), infundibulum (arrow), and arcuate nucleus (ARC). (*B*) Dark-field photomicrograph of parasagittal section of the brainstem and cerebellum from 18-week-old transgenic mouse from line 3 (×7.5). Silver-grain density is greatest over cerebellar Purkinje cells (PC), lateral vestibular nucleus (LVe), red nucleus (R), motor nucleus of the fifth and seventh cranial nerve (Mo5 and Mo7, respectively), and deep areas of the superior and inferior colliculi (SC and IC, respectively).

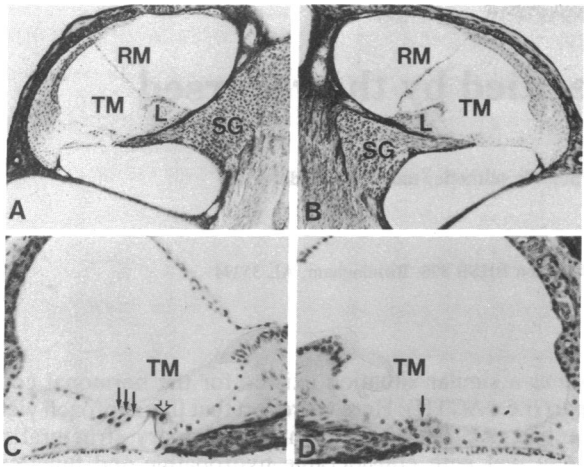

FIG. 4. Pathology of inner ears (middle turn of the cochlea) transgenic mice from line 3 and control littermates. (*A*) Control mouse (×60). Note the densely packed spiral ganglion cells. (*B*) Transgenic mouse (×60). The spiral ganglion is less densely populated than in control animals. The limbus is flattened on surface normally abutting Reissner's membrane. (*C*) Control mouse (×120). There are three distinct outer hair cells (solid arrows) with the tectorial membrane attached and a single distinct inner hair cell (open arrow). (*D*) Transgenic mouse (×120). There is total loss of inner and all outer hair cells and their supporting cells, with detachment of tectorial membrane from the residual mound of cellular debris (arrow). SG, spiral ganglion; TM, tectorial membrane; L, Limbus; RM, Reissner's membrane.

(Fig. 4). The mice failed to show any reaction to the startle–response test. Brain stem auditory-evoked potential recordings revealed total absence of any brain stem auditory-evoked potential waveform, even at maximal stimulus intensity (data not shown).

DISCUSSION

Concomitant with high transgene expression, *Mos* transgenic mice develop progressive lesions in several areas of the brain involving neurons and glial cells. In addition, we observe inflammatory infiltrates, presumably related to a breakdown in the blood–brain barrier, which could represent an autoimmune-like response or might be due to the synthesis and release of some chemotactic factor (e.g., interleukin 1) by the neurons and glia. The clinical features of ataxia and loss of startle response in transgenic mice can be attributed to cerebellar degeneration, loss of hair cells, and degeneration of spiral ganglia. The latter defects are reminiscent of those defects found in many mouse spotting mutants (25).

The lesions we have observed in the brain and lens-fiber epithelial cells (16) may be due to a block in cellular differentiation or a failure to maintain the synthesis of gene products necessary to maintain the differentiated state. In *Mos* transgenic animals, the inability of committed lens cells to enucleate and subsequently to become transparent (16), the retraction and degeneration of the neuronal fibers, the unusual nuclei found in some brain cells, and the multinucleated astrocytes might be related to the role that *Mos* plays in meiosis. Our findings resemble the interference of other oncogenes with cellular differentiation. For example, constitutive expression of the c-*myc* oncogene in mouse erythroleukemia cells blocks their ability to differentiate (26). Likewise expression of the polyoma large tumor antigen in lens cells of transgenic mice perturbs lens-cell differentiation (27). We show that *Mos* is expressed in the brain during early development, suggesting that its target and substrates are present in this tissue. Overexpression of the *Mos* protein serine/threonine kinase might disturb the intricate balance of protein phosphorylation that regulates cellular differentiation and function, particularly in the brain (28). We have determined that tubulin associates with the *Mos* protooncogene product *in vivo* and can be specifically phosphorylated by $pp39^{mos}$ kinase *in vitro* (29), suggesting that *Mos* may function in the modification of tubulin and thereby affect neuronal cells.

This research was sponsored in part by the National Cancer Institute, Department of Health and Human Services, under Contract N01-CO-74101 with ABL, and National Institutes of Health Grants NS20820, GM20919, and RR01183.

1. Propst, F., Rosenberg, M. P., Iyer, A., Kaul, K. & Vande Woude, G. F. (1987) *Mol. Cell. Biol.* **7**, 1629–1637.
2. Propst, F. & Vande Woude, G. F. (1985) *Nature (London)* **315**, 516–518.
3. Propst, F., Rosenberg, M. P., Oskarsson, M. K., Russell, L. B., Nguyen-Huu, M. B., Nadeau, J., Jenkins, N. A., Copeland, N. G. & Vande Woude, G. F. (1988) *Oncogene* **2**, 227–233.
4. Goldman, D. S., Kiessling, A. A., Millette, C. F. & Cooper, G. M. (1987) *Proc. Natl. Acad. Sci. USA* **84**, 4509–4513.
5. Mutter, G. L. & Wolgemuth, D. J. (1987) *Proc. Natl. Acad. Sci. USA* **84**, 5301–5305.
6. Keshet, E., Rosenberg, M. P., Mercer, J. A., Propst, F., Vande Woude, G. F., Jenkins, N. A. & Copeland, N. G. (1988) *Oncogene* **2**, 235–240.
7. Paules, R. S., Propst, F., Dunn, K. J., Blair, D. G., Kaul, K., Palmer, A. E. & Vande Woude, G. F. (1988) *Oncogene* **3**, 59–68.
8. Schmidt, M., Oskarsson, M. K., Dunn, J. K., Blair, D. G., Hughes, S., Propst, F. & Vande Woude, G. F. (1988) *Mol. Cell. Biol.* **8**, 923–929.
9. Sagata, N., Oskarsson, M., Copeland, T., Brumbaugh J. & Vande Woude, G. F. (1988) *Nature (London)* **335**, 519–525.
10. Paules, R. S., Buccione, R., Moschel, R. C., Vande Woude, G. F. & Eppig, J. J. (1989) *Proc. Natl. Acad. Sci. USA* **86**, 5395–5399.
11. Herzog, N. K., Singh, B., Elder, J., Lipkin, I., Trauger, R. J., Millette, C. F., Goldman, D. S., Wolfes, H., Cooper, G. M. & Arlinghaus, R. B. (1988) *Oncogene* **3**, 225–229.
12. O'Keefe, S. J., Wolfes, H., Kiessling, A. A. & Cooper, G. M. (1989) *Proc. Natl. Acad. Sci. USA* **86**, 7038–7042.
13. Freeman, R. S., Pickham, K. M., Kanki, J. P., Lee, B. A., Pena, S. V. & Donoghue, D. J. (1989) *Proc. Natl. Acad. Sci. USA* **86**, 5805–5809.
14. Sagata, N., Daar, I., Oskarsson, M., Showalter, S. D. & Vande Woude, G. F. (1989) *Science* **245**, 643–645.
15. Sagata, N., Watanabe, N., Vande Woude, G. F. & Ikawa, Y. (1989) *Nature (London)* **342**, 512–518.
16. Khillan, J. S., Oskarsson, M. K., Propst, F., Kuwabara, T., Vande Woude, G. F. & Westphal, H. (1987) *Genes Dev.* **1**, 1327–1335.
17. Osborn, L., Rosenberg, M. P., Keller, S. A. & Meisler, M. H. (1987) *Mol. Cell. Biol.* **7**, 326–334.
18. Southern, E. (1975) *J. Mol. Biol.* **98**, 503–517.
19. Fink, R. P. & Heimer, L. (1967) *Brain Res.* **4**, 369–374.
20. Cork, L. C., Troncoso, J. C., Klavano, G. G., Johnson, E. S., Sternberger, L. A., Sternberger, N. H. & Price, D. L. (1989) *J. Neuropathol. Exp. Neurol.* **47**, 420–431.
21. Chomczynski, P. & Sacchi, N. (1987) *Anal. Biochem.* **162**, 156–159.
22. Melton, D. A., Krieg, P. A., Rebagliati, M. R., Maniatis, T., Zinn, K. & Green, M. R. (1984) *Nucleic Acids Res.* **12**, 7035–7056.
23. Hogan, B., Constantini, F. & Lacy, E. (1986) *Manipulating the Mouse Embryo: A Laboratory Manual* (Cold Spring Harbor Lab., Cold Spring Harbor, NY).
24. Blair, D. G., Oskarsson, M., Wodd, T. G., McClements, W. L., Fischinger, P. J. & Vande Woude, G. F. (1981) *Science* **212**, 941–943.
25. Steel, K. P., Niaussat, M. M. & Bock, G. R. (1982) in *The Auditory Psychobiology of the Mouse*, ed. Willot, J. F. (Thomas, Springfield, IL), pp. 341–394.
26. Coppola, J. A. & Cole, M. (1986) *Nature (London)* **320**, 760–765.
27. Griep, A. E., Kuwahara, T., Lee, E. J. & Westphal, H. (1989) *Genes Dev.* **3**, 1075–1085.
28. Nestler, E. J. & Greengard, P. (1984) *Protein Phosphorylation in the Nervous System* (Wiley, New York).
29. Zhou, R., Oskarsson, M., Paules, R. S., Schulz, N. & Cleaveland, D. (1990) *Science*, in press.